Mixed-Mode Fiber Array Alignment and Coupling to Photonic Integrated Circuits

Kamil Gradkowski

***Abstract*—This study investigates alignment and coupling between a photonic integrated circuit (PIC) and a mixed-mode fiber array, where one of the channels in the normally single-mode (SM) array is replaced by a multi-mode fiber (MMF). As a result, the tolerances of alignment are significantly relaxed. The proposed method suggests using the SMF at the input and the MMF at the output of the PIC. In such a transmission configuration, the tolerances are relaxed by a factor of √2 (41%). As this scales with mode size, the beam-expansion mechanisms, e.g., utilizing micro-lenses, can further significantly reduce the requirements for fabrication and packaging of photonic devices, making them more robust and cheaper to manufacture.**

***Index Terms*— Photonic integrated circuits, edge couplers, micro-optical devices, expanded-beam optical connectors**

I. Introduction

PHOTONIC integrated circuits (PICs) are undergoing a period of rapid development as an optical counterpart of the electronic ICs. Their potential lies in a broad range of applications and low power consumption coupled with high sensitivity [1]. Coupling optical signals into and out of the PICs is however very difficult and requires high precision, of the order of single microns [2]. This is due to the fact that the waveguides on the PIC are designed to be single-mode (multi-mode designs exist, but not very prevalent [3]) and the mode-field diameter (MFD) at the output coupler can be as small as 3µm (or even smaller) [4], but will be no larger than the corresponding MFD of the single-mode fiber (SMF) that is used to couple light, e.g., 9.2µm at 1310nm or 10.4µm at 1550nm for an SMF-28 fiber. Recent work [5] showed that in a mode-matched situation the alignment tolerances, defined as a displacement from the optimal position where additional coupling losses exceed 1dB, are 0.24 of the MFD. Such a restrictive accuracy requirement, especially across an array of fibers, is a unique technical challenge that is associated with photonic packaging and it leads to increased costs [6] in comparison to its' electronic counterpart. Multi-mode fibers (MMFs) are utilized in photonics for this specific reason, however their use is currently relegated to short-haul data communication in data centers [7][8] by coupling them to vertical cavity surface emitting lasers (VCSELs) [9].

Recent efforts in photonics packaging that intend to address the tolerance issue are focused on expanding the mode between the PIC and the fiber using micro-optics [10][11][12][13]. It was demonstrated that by expanding the beam by a factor of 5-10 one can construct a robust pluggable single-mode direct optical connector device, which can streamline the packaging process.

This paper investigates the advantages of utilizing MMFs for photonic IC packaging, primarily in conjunction with micro-optic beam expansion scheme. This method can be used in any application that relies primarily on measurement of the signal intensity at the output of the chip, e.g., for aforementioned short-haul data communications. However, the primary beneficiary could be in sensing applications. One of the more common on-chip implementations of a sensor utilizes phase detection using, e.g., a Mach-Zehnder interferometer [14], where one arm of the sensor is sensitive to the change in the environment resulting in phase shift between the arms that translates into a change in signal intensity. Such sensors were shown to detect chemical molecules [15], but also temperature [16]. Another type is a Raman-scattering-based sensors [17]. While very selective, they require long waveguides due to poor conversion efficiency [18]. Such applications could benefit from MMF coupling in several ways: (1) larger core of the MMF means that typically more light can be captured than by the SMF, lowering the power requirements of the device; (2) tolerances of alignment of the fiber to the chip would be further relaxed; (3) in conjunction with the pluggable aspect of the expanded beam scheme, field-replaceable sensors can be deployed. While detectors can be integrated onto the PIC to locally measure the signal intensity [19], fully passive sensors that utilize transmission of light, i.e., rely on external light source and a measurement interrogator, can be more robust and easier to package; therefore, fabricated at a lower cost and in a more scalable manner.

II. Experiment Details

A. Reference PIC and Fiber Array

The PIC used in this work is a SiN-based reference structure fabricated by Lionix®. It contains several short loopbacks connecting edge couplers pitched at 250µm. Fig. 1(a) shows a layout of the structure. 3 loopbacks are used in the experiments. This fairly represents the state-of-the-art packaging process, where the outer channels are used for precise correction of roll and alignment of the entire array [2] and the active channels are positioned in the middle. The size of the coupler mode size is determined to be 6.8x6.2µm [11] at 1550nm. The PIC edge is stealth-diced [21] to create a low-

Manuscript received: xx-xx-xxxx. This work was supported by Taighde Éireann – Research Ireland (grant no. SFI-12/RC/2276_P2).

K. Gradkowski is with Tyndall National Institute, Lee Maltings, T12 R5CP, Cork, Ireland (e-mail: kamil.gradkowski@tyndall.ie).

This article has been accepted for publication in IEEE Transactions on Components, Packaging and Manufacturing Technology. This is the author's version which has not been fully edited content may change prior to final publication. Citation information: DOI 10.1109/TCPMT.2025.3560722

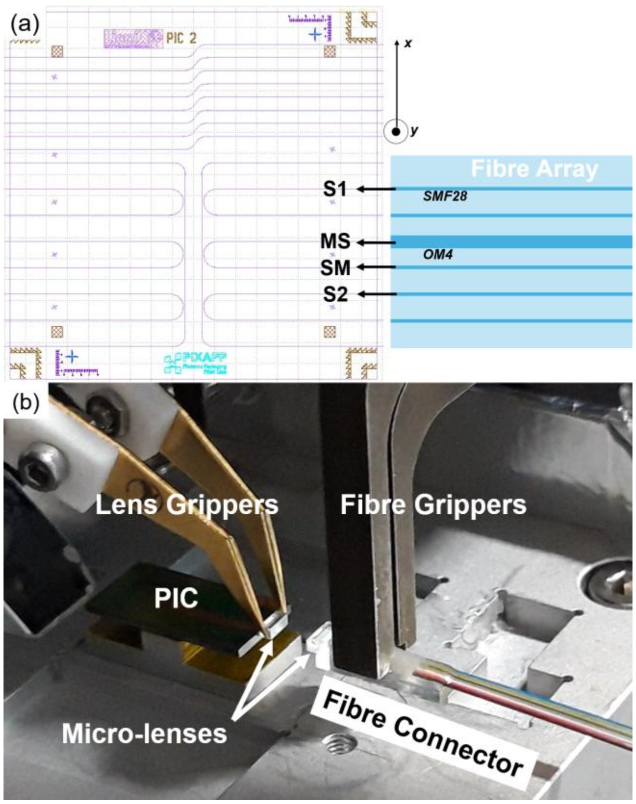

Fig. 1 (a) Schematic of the reference PIC and the fiber array design. (b) Photograph of the lens alignment procedure.

loss facet.

The fiber array is fabricated to match the PIC design. It is composed of 6 channels, 5 of which are SMF28 standard single-mode fiber, while one (channel #3) is fitted with OM4 multi-mode fiber. This fiber is commonly used in short-haul LAN networks and has a core 50µm in diameter. Fig. 1(a) shows schematically the layout of the fiber array (FA) against the PIC. The two outer channels have all-single-mode input and output and are labeled S1 and S2 respectively (or S-channels collectively). The inner path is asymmetric due to the presence of the MMF; therefore, the light routing direction is important. Where the light is injected using the single-mode channel and is detected using multi-mode channel, the path is labeled SM. The opposite route is labeled MS. Note that the MS route would not be normally used in the device operation, since the launch conditions (i.e., the modal configuration at the fiber output) are essentially random and subject to significant variability. The variability stems from coupling between higher-order modes in the MMF and can be suppressed by reducing fiber length, limiting stress caused by bends, as well as favorable launch conditions that excite as few higher modes as possible [21]. As such, it is included for comparison purposes only.

B. Micro-lenses

For a thorough investigation of the effect of various parameters on the performance of the contactless optical link, 2 different off-the shelf lens designs are utilized. All lenses used in this study are made from fused silica and are plano-convex to be able to attach one side to the PIC. The first lens (abbreviated Lens A) is fabricated by Axetris®. It has a thickness of 1mm and a radius of curvature (ROC) of 315µm. It possesses an anti-reflection (AR) coating on both sides, optimized for operation in air. This lens was utilized in previous work on pluggable connector in a grating coupler paradigm [10]. Two lenses are utilized for the demonstration – one attached to the fiber, the other aligned to the PIC. When aligned to a SMF with a mode-field diameter (MFD) of 10.4µm, it produces a collimated beam 135µm in diameter. When placed on the PIC however, the beam exhibits a calculated elliptical profile 206x227µm in size. This mode mismatch is one of the primary sources of optical losses in the link.

The second lens design, fabricated by Focuslight (Lens B), is similar to Lens A. It is 1mm thick with an ROC of 325µm, producing 213x234µm-wide beam on the PIC side and 139µm MFD beam on the SMF side. The major difference from the Lens A design is the AR coating, which is only placed on the lens (i.e., front) side. This reduces reflections to a minimum when an index-matched liquid or an adhesive is placed in the optical path. Similarly to the previous configuration, two B lenses are placed on both sides of the optical interface.

C. Experimental Procedure

The optical alignment procedure is performed on a nanosystec® NanoGlue system, equipped with two 6-axis stages which allow for high-precision alignment (better than 0.1µm translation and 0.005° rotation). Both experiments involving lenses require first an attachment of the lens to the FA. This is performed using an optical fiber circulator to direct light to the fiber and measuring the returning signal [13]. The light passes through the fiber, the lens and is bounced back from a mirror positioned a small distance (3.5mm) away from the facet. The position of the lens is optimized to maximize the returning signal on all channels of the array. The light source is a 1550nm Thorlabs® S5FC1550S-A2 broadband SLD. The lens is fixed to the FA facet using Dymax® OP-4-20632 UV-curable adhesive, forming a fiber connector assembly.

The connector is then used to optimize the position of the lens that couples the light into the PIC. Both S-channels are utilized to actively align the lens along all 6 axes to ensure uniformity across the array [22]. A photograph of this alignment procedure is shown in Fig. 1(b). The lens is not attached to the chip since the same PIC is used for all experiments for comparison.

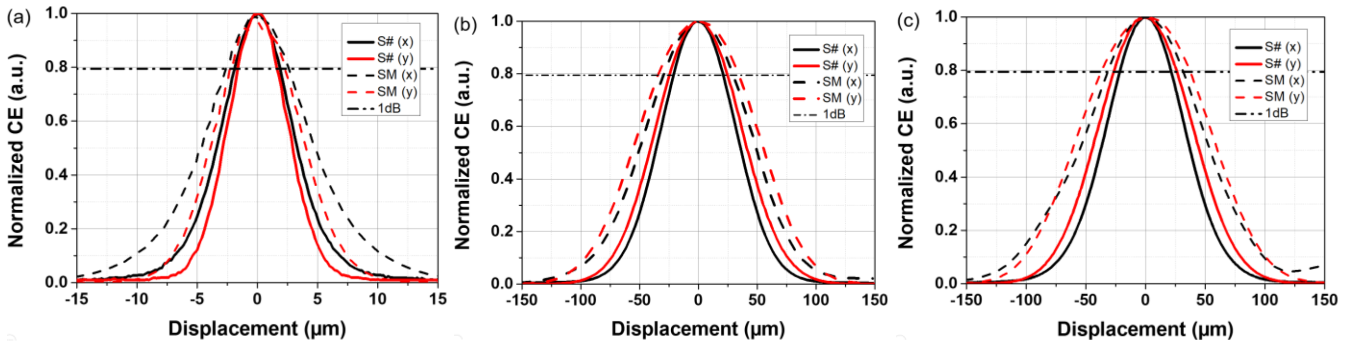

Fig. 2 Alignment tolerance curves for (a) reference FA displacement, and (b) Lens A, (c) Lens B fiber connector displacements. Black curves correspond to x-axis, red – to y-axis. Solid lines are recorded on one of the S-channels, while dashed line represents the SM channel. Horizontal line shows 1dB tolerance cut-off level.

There are two critical parameters evaluated in this work. One of them is the displacement tolerance, which is measured by displacing the fiber array, the PIC lens or the lens-equipped fiber connector from its' optimal position. The numeric value is assigned to the displacement at which the additional optical losses exceed 1dB. As the MFD of the PIC is asymmetric, so the tolerances are also expected to be axis-dependent. As shown in Fig. 1(a) the x-axis is along the PIC edge, while the y-axis is normal to the PIC surface.

The other metric of evaluation is the optical transmission loss through the loopback. While previous works concentrated on measuring coupling efficiency per-coupler [10][11][13], the overall transmission is a more relevant parameter, since it directly measures the expected signal integrity of a packaged device operating in light transmission mode.

III. Results and Discussion

A. Reference Measurement

The reference measurement positions the bare fiber array directly against the PIC facet. It gives a baseline for comparison for the following methods as well as provides insight into the possible improvements to the operation in situations where the fiber array is directly bonded to the PIC. The transmission loss through the S1 and S2 channels is measured at 2.66dB and 2.86dB respectively. The SM path shows improved transmission of 1.83dB, an improvement of 0.8-1dB over the single-mode channels. The MS channel exhibits on the other hand much higher losses at 3.9dB. That the losses in this case are not much higher, as could be predicted from the substantial mode mismatch between the MMF and the PIC output coupler, is attributed to a short length of the fiber (1m) and the fact that it is not significantly bent, which limits the power transfer to the higher-order modes.

The tolerances of alignment are shown in Fig. 2(a). The solid lines represent one of the S-channel tolerances, while the dashes represent the SM channel. Black curves are displacement in the horizontal (x) direction, while red curves – vertical (y) direction. The horizontal line in Fig. 2 depicts a 1dB tolerance threshold. The alignment tolerance to the standard single-mode loopback is 1.9x1.64µm. The MS channel (not shown) has a tolerance of 2.12x1.79µm. The SM channel has tolerance of 2.61x2.3µm, which is a significant improvement. In all cases the tolerance in the vertical direction is smaller than in the horizontal, because the PIC mode is smaller on that axis.

B. Micro-lens A

In this configuration, the transmission loss through the S1 and S2 channels is 3.99dB and 4.25dB respectively. The MS channel exhibits higher losses at 4.83dB, while the SM channel improves the signal to 3.28dB. The higher losses in the S-channels, between 1.33dB to 1.39dB, as compared to the reference measurement, are a result of the aforementioned expanded mode mismatch that occurs in the air gap. Similarly to the reference measurement, we observe an improvement of the transmission when using the MMF at the output.

The tolerances of alignment are divided into two sections when using micro-lenses. One is the alignment tolerance of the PIC lens itself. The values here are similar, albeit slightly lower than the tolerances of alignment of the fiber array to the PIC with differences being of the order of 0.1µm. Most important however are the tolerances of alignment of the fiber array assembly, which are responsible for a contactless, pluggable operation. These are shown in Fig. 2(b). Thanks to beam expansion, the alignment tolerance for the S-channel is 21.2x24.7µm. This order-of-magnitude improvement is a result of >10-fold expansion of the mode in comparison with the PIC-to-fiber direct connection [11]. The tolerance is higher in the vertical (y) direction, since the mode from the PIC has higher divergence in that direction, which leads to a larger expanded mode size. The MS channel tolerances are 19.1x22.5µm, while the SM channel shows further significant improvement to 29.7x34.5µm, a 40% increase as compared to the S-channel.

C. Micro-lens B

In this configuration the losses in air are quite similar to Lens A, 3.69dB for both S-channels, 4.58dB for MS and 3.14dB for SM channel respectively. With an index-matched liquid placed in the optical path, the transmission loss becomes very similar to the reference measurement, with 2.48 and 2.7dB for S1 and S2 respectively, 3.43dB for the MS and 1.96dB for the SM channel due to reduction of reflections.

This article has been accepted for publication in IEEE Transactions on Components, Packaging and Manufacturing Technology. This is the author's version which has not been fully edited content may change prior to final publication. Citation information: DOI 10.1109/TCPMT.2025.3560722

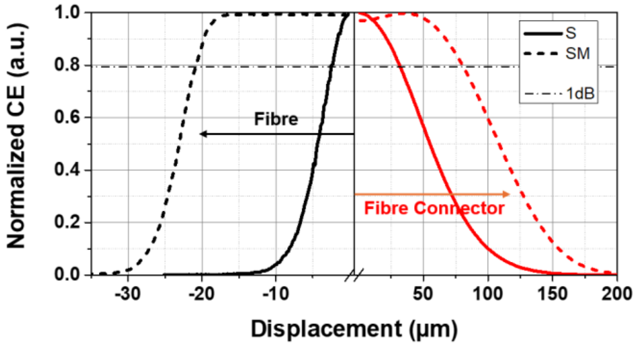

Fig. 3 Displacement tolerance curves in fiber-to-fiber (black, left-hand side) and lensed-fiber to lensed-fiber (red, right-hand side) experiments. Solid line represents SMF to SMF injection and the dashed – SMF to MMF. The horizontal line shows 1dB tolerance cut-off.

The tolerances of alignment of the PIC lens are 0.1-0.3µm better than the reference measurement. Similarly to the other configuration, the tolerances of displacement of the connector, as depicted in Fig. 2(c), show great improvement. The value for S-channels is similar to lens A: 21.6x26.5µm due to similar size of the expanded mode. The MS channel has tolerances of 19x.24.7µm, while the SM channel: 31.6-37.2µm, more than 40% improvement over the regular S-channels.

D. Discussion

In all presented cases we observe a significant increase in alignment tolerances (~40%) when the light is injected using a single-mode fiber and detected using a multi-mode fiber, as compared to the single-mode symmetrical I/O arrangement. The values are summarized in Table I.

Fig. 3 provides a straightforward explanation for the observed phenomena. It shows results of an independent experiment conducted in two parts. In the first, two bare fiber arrays are aligned face-to-face, and a displacement tolerance is measured for coupling from SMF to SMF (solid black line) and from SMF to MMF (dashed black line). The results are shown on the left-had side of the graph. In the second part, two fiber arrays with an attached Lens A are positioned opposite one another and the same displacement measurement is performed. The results are displayed on the right-hand side of the graph. As the fiber modes are symmetrical, only one axis is shown.

The tolerances of alignment of a SMF to the same SMF without a micro-lens are 2.5µm [5]. When two single-mode channels are involved in alignment, e.g. through a loopback, the curve is effectively squared leading to a reduced tolerance, as is observed in the experiment. However, the MMF has a flat acceptance curve for about 70% of the 50µm core size. This means that the response of the system only depends on the size of the single mode, leading to significantly relaxed alignment tolerances.

Similar effects are observed with micro-lenses at the interface. The expansion of the beam to 135µm leads to a significant relaxation of the base SMF-SMF alignment tolerance (solid red line). The measured value of 32.2µm is in excellent agreement to the theoretical value for aligned Gaussian beams of 32.4µm [5]. For SM-MM coupling through the lens doublet we observe further, significant relaxation of the alignment tolerance (to 80.7µm) with a difference that the coupling efficiency is not highest at the center. The peak coupling occurs (for the lenses and fibers utilized in the experiment) around 35µm off-center, but the difference amounts only to 3%, or 0.13dB. This is due to the fact that the beam hitting the lens off-center will skew the rays [10] and inject light into skew modes of the MMF [23][24].

The obtained tolerance enhancement (scaling) factor (80.7µm against 32.2µm) is 2.5, which is much larger than that observed in the experiments involving the PIC, where the improvement is only around 1.4 (this is shown in parentheses in Table I). The interpretation of this fact has to again take into account that in the first case we are analyzing a direct, single-channel translation tolerance, while the translation against the loopbacks on the PIC involves displacement against two couplers, which effectively squares the field. Applying the square operation to the data in Fig. 3 (solid red line), the resulting alignment tolerance is 22.64µm, which is a factor 1.42 smaller than the original 32.2µm. This demonstrates that the MMF at the output effectively reduces the problem of packaging to matching two single-mode channels together. The improvement factor is equal to $\sqrt{2}$ and is independent of the size of the mode, meaning that the more the beam is expanded using micro-lenses, the greater the benefit from utilizing the presented method. Small differences in this factor, as is shown in Table I, can be due to measurement accuracy or the asymmetry of the optical coupling system, i.e., when the expanded beam modes are not matched.

The improvements in alignment tolerances correlate with improved optical transmission through the various channels. Table II summarizes the results, excluding the MS channel. The Δ corresponds to a difference between the SM channel and the average transmission loss through the S-channels. For the reference measurement using a butt-coupled fiber, the improvement is close to 1dB. This is due to a greater modal cross-section of the MMF core that corresponds to a larger

Table I: Measured alignment tolerances for all experimental configurations. MS channels are excluded. Values in parentheses show the calculated tolerance enhancement factor which is a ratio of SM to S-channel tolerance for each direction.

Configuration		Alignment Tolerances [µm]	
		x (*enh. fact.*)	**y (*enh. fact.*)**
Reference	S	1.9	1.64
	SM	2.61 (1.37)	2.3 (1.4)
Lens A	S	21.2	24.7
	SM	29.7 (1.4)	34.5 (1.4)
Lens B	S	21.6	26.5
	SM	31.6 (1.46)	37.2 (1.4)

Table II: Measured transmission losses for all experimental configurations. MS channels are excluded. Δ corresponds to difference between SM and the averaged S-channels.

Configuration	Transmission Losses[dB]		
	S (avg.)	SM	Δ
Reference	2.76	1.83	-0.93
Lens A	4.12	3.28	-0.84
Lens B (Air)	3.69	3.14	-0.55
Lens B (IML)	2.59	1.96	-0.63

numerical aperture (0.2 for OM4 fiber compared to 0.14 of SMF-28 fiber) and relaxes the light injection requirements from an output coupler that exhibits larger beam divergence due to a smaller MFD. Additionally, the impact of the fiber array manufacturing tolerances (e.g., v-groove pitch variation and core concentricity) is reduced.

A similar situation occurs when the micro-lenses are employed in the optical path. ZEMAX simulation of the Lens B configuration with an index-matching liquid in all-SM transmission gives a roundtrip loss of 2.51dB, which is caused by the significant mode mismatch in the air gap and is in reasonable agreement with the measurement. The excess losses for Lens A and Lens B in air are likely the effect of surface roughness of the PIC facet, as well as the reflections on the back facet of the lens, which are both negated by the presence of the liquid [11]. On average, in the experiment with an OM4 fiber at the output we observe an improvement in transmission of between 0.55dB and 0.84dB when compared to an all-SM path, as the larger fiber core can capture more light from a mode-mismatched expanded beam re-focused by the fiber lens. However, the overall coupling efficiency can be better improved with non-off-the-shelf PIC micro-lenses that are specifically designed to match the fiber connector expanded mode, which will diminish any further improvement in optical coupling stemming from using the MMF. For example, a 650µm-thick fused silica lens with a 212µm ROC placed on the PIC provides good mode-matching with a Lens B design on the fiber. The simulated roundtrip losses through one of the S-channels are in such a case <0.3dB and mostly stem from the asymmetry of the PIC mode. Therefore, in expanded beam interconnects the primary benefit lies in the increased alignment tolerances.

IV. Conclusion

The results presented in this study demonstrate that there are no practical drawbacks to using an MMF at the output of the fiber array in all applications that are based on the measurement of the amplitude of optical signal transmitted through – or outcoupled from – the PIC. Transmission increases by 0.55dB – 0.93dB for all investigated cases in comparison to the regular SM-SM path. More importantly, and critically for packaging, the alignment tolerances are relaxed by a factor of $\sqrt{2}$, leading to loosened manufacturing and assembly requirements, which typically translates into faster packaging and cheaper devices [1]. Using micro-lenses to expand the beam leads to further and significant relaxation of alignment tolerances between the connector and the PIC assembly, making pluggable solutions easier to deploy and the devices cheaper to manufacture. It has to be noted however, that the alignment of the individual lens to the PIC has very similar tolerances to alignment of the fiber.

References

[1] L. Ranno *et al.*, “Integrated Photonics Packaging: Challenges and Opportunities,” *ACS Photonics* vol. 9, no. 11, pp. 3467–3485, 19 Oct. 2022, doi: 10.1021/acsphotonics.2c00891.

[2] R. Marchetti, C. Lacava, L. Carroll, K. Gradkowski and P. Minzioni, "Coupling strategies for silicon photonics integrated chips [Invited]," *Photon. Res*. vol. 7, pp. 201-239, 31 Jan. 2019, doi: 10.1364/PRJ.7.000201.

[3] L. Zheng, U. Zywietz, T. Birr, M. Duderstadt, L. Overmeyer, B. Roth and C. Reinhardt, “UV-LED projection photolithography for high-resolution functional photonic components,” *Microsyst. Nanoeng. vol.* **7**, p. 64, 17 Aug. 2021, doi: 10.1038/s41378-021-00286-7.

[4] L. Carroll, *et al.*, “Photonic Packaging: Transforming Silicon Photonic Integrated Circuits into Photonic Devices,” *Appl. Sci.* vol. *6*, p. 426, 15 Dec. 2016, doi: 10.3390/app6120426.

[5] K. Gradkowski, "Tolerances of the alignment of fibers to photonic integrated circuits," *Appl. Opt.* vol. 63, pp. 8407-8412, 7 Nov. 2024, doi: 10.1364/AO.540682

[6] T. Barwicz *et al*., "A Novel Approach to Photonic Packaging Leveraging Existing High-Throughput Microelectronic Facilities," *IEEE Journal of Selected Topics in Quantum Electronics*, vol. 22, no. 6, pp. 455-466, 20 Jul. 2016, doi: 10.1109/JSTQE.2016.2593637.

[7] Y. Koike and S. Takahashi, “Plastic optical fibers: technologies and communication links,” in *Optical Fiber Telecommunications VB: Systems and Networks*, pp. 593-603, I. P. Kaminow, T. Li and A. E. Willner eds. (Elsevier Academic, 2008).

[8] A.F. Benner, M. Ignatowski, J.A. Kash, D.M. Kuchta and M.B. Ritter, "Exploitation of optical interconnects in future server architectures," *IBM Journal of Research and Development* vol. 49, no. 4.5, pp. 755-775, July 2005, doi: 10.1147/rd.494.0755.

[9] J.A. Tatum *et al*., "VCSEL-Based Interconnects for Current and Future Data Centers," *J. of Lightwave Technology*, vol. 33, no. 4, pp. 727-732, 15 Feb. 2015, doi: 10.1109/JLT.2014.2370633.

[10] C. Scarcella *et al.*, "Pluggable Single-Mode Fiber-Array-to-PIC Coupling Using Micro-Lenses," *IEEE Photonics Technology Letters*, vol. 29, no. 22, pp. 1943-1946, Nov. 2017, doi: 10.1109/LPT.2017.2757082.

[11] K. Gradkowski, D. Stegall, D. Mackey, A. Naughton, T. Smith and P. O'Brien, "Demonstration of a Single-Mode Expanded-Beam Connectorized Module for Photonic Integrated Circuits," *J. of Lightwave Technology*, vol. 41, no. 11, pp. 3470-3478, Jun. 2023, doi: 10.1109/JLT.2023.3239138.

[12] Y. Du, F. Wang, Z. Hong, Y. Shi, X. Chen and X Zheng, "Detachable interface toward a low-loss reflow-compatible fiber coupling for co-packaged optics (CPO)," *Opt. Express* vol. 31, pp. 1318-1329, 3 Jan. 2023, doi: 10.1364/OE.480418.

[13] K. Gradkowski *et al*., "Solder Reflow Resistant Thermoplastic for Optical Coupling," *IEEE Transactions on Components, Packaging and Manufacturing Technology*, 23 Jan. 2025, doi: 10.1109/TCPMT.2025.3532026

[14] J. Milvich, D. Kohler, W. Freude and C. Koos, "Integrated phase-sensitive photonic sensors: a system design tutorial," *Adv. Opt. Photon.* vol. 13, pp. 584-642, 3 Sep. 2021, doi: 10.1364/AOP.413399.

[15] H. Niu, *et al.*, "Mach-Zehnder interferometer based integrated-photonic acetone sensor approaching the sub-ppm level detection limit," *Opt. Express* vol. 30, pp. 29665-29679, 29 Jul. 2022, doi: 10.1364/OE.459805.

[16] G. Li, T. Li, Y. Liu and Y. Zheng, “A new Mach–Zehnder interference temperature measuring sensor based on silica-based chip,” *Sci. Rep.* vol. 14, p. 8657, 15 Apr. 2024, doi: 10.1038/s41598-024-59447-z.

[17] D.M. Kita, J. Michon, and J.J. Hu, "A packaged, fiber-coupled waveguide-enhanced Raman spectroscopic sensor," *Opt. Express* vol. 28, no. 10, pp. 14963-14972, 1 May 2020, doi: 10.1364/OE.392486.

[18]A. Dhakal, A.Z. Subramanian, P. Wuytens, F. Peyskens, N. Le Thomas, and R. Baets, "Evanescent excitation and collection of spontaneous Raman spectra using silicon nitride nanophotonic waveguides," *Opt. Lett.* vol. 39, pp. 4025-4028, 30 Jun. 2014, doi: 10.1364/OL.39.004025.

[19]P. Su, Z. Han, D. Kita, P. Becla, H. Lin, S. Deckoff-Jones, K. Richardson, L. C. Kimerling, J. Hu and A. Agarwal, "Monolithic on-chip mid-IR methane gas sensor with waveguide-integrated detector," *Appl. Phys. Lett.* vol. 114, no. 5, p. 051103, 4 Feb. 2019, doi: 10.1063/1.5053599.

[20]M. Kumagai, N. Uchiyama, E. Ohmura, R. Sugiura, K. Atsumi and K. Fukumitsu, "Advanced Dicing Technology for Semiconductor Wafer—Stealth Dicing," *IEEE Transactions on Semiconductor Manufacturing*, vol. 20, no. 3, pp. 259-265, Aug. 2007, doi: 10.1109/TSM.2007.901849.

[21]J.N. Kutz, J.A. Cox and D. Smith, "Mode Mixing and Power Diffusion in Multimode Optical Fibers," *J. Lightwave Technol.* vol. 16, p. 1195, Jul. 1998.

[22]K. Gradkowski, P.E. Morrissey and P. O'Brien, "Packaging of micro-lens arrays to photonic integrated circuits using beam shape evaluation," *J. Phys. Photonics* vol. 6, p. 035022, 3 Jul. 2024, doi: 10.1088/2515-7647/ad5bd2.

[23]X.H. Zhao, and Y. Gao, "Effect of injection misalignment on multimode fiber power delivery characteristics," *Acta Photonica Sinica*, vol. 37, no. 9, pp. 1842-1847, Sep. 2008.

[24]G.Y. Chen, J. Wang, and D.G. Lancaster, "Fiber-Optic Skew Ray Sensors" *Sensors*, vol. 20, no. 9, p. 2499, Apr. 2020, doi: 10.3390/s20092499.